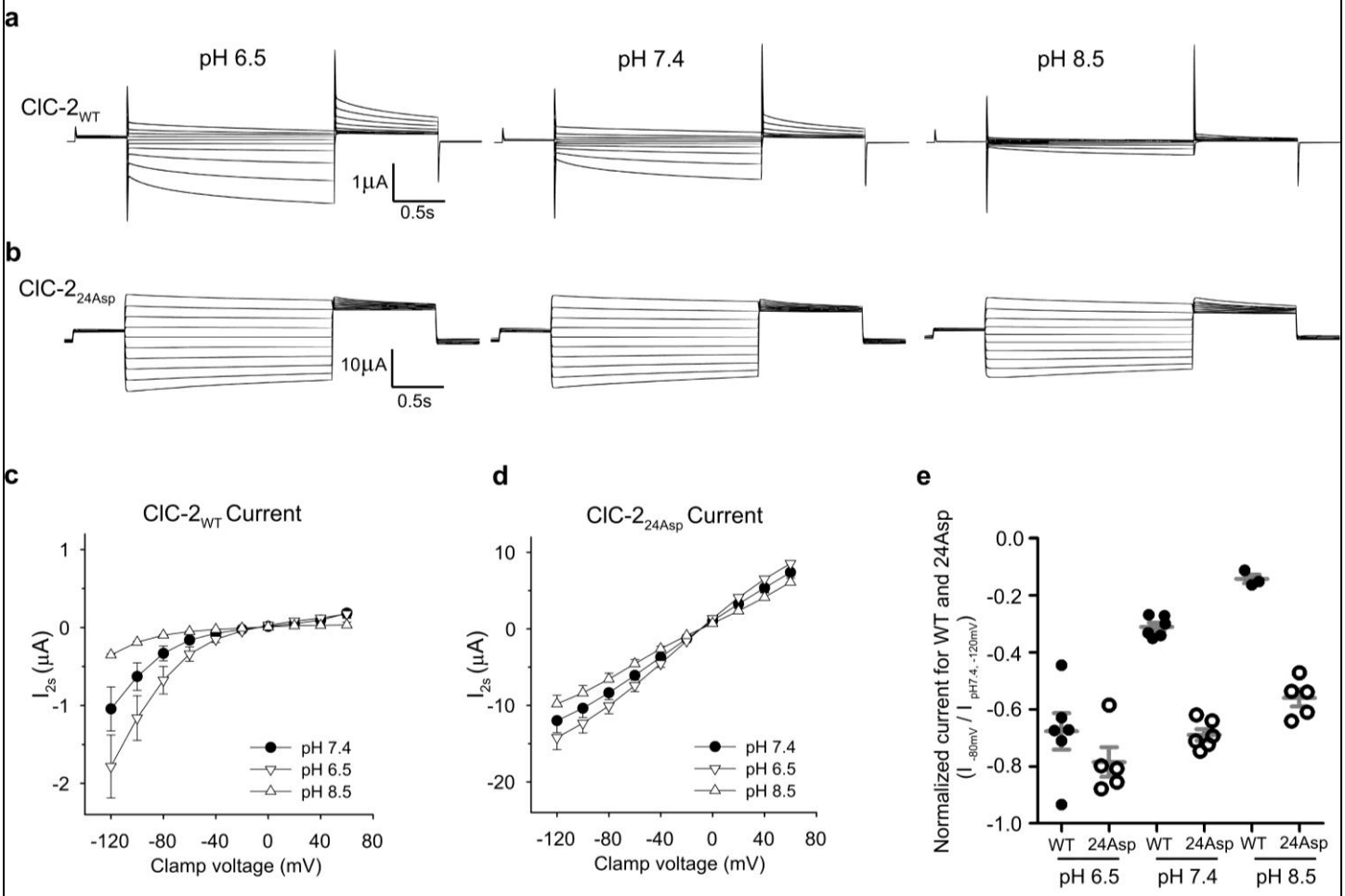

Supplementary Figure 1

Dependence of ClC-2$_{WT}$ and ClC-2$_{24Asp}$ currents on external pH.

WT and mutant channels were expressed in *Xenopus* oocytes and measured by two-electrode voltage-clamp using a pulse protocol that clamped the oocytes in 2-s long, 20 mV steps from + 50 to -120 mV. (a, b) Representative current traces obtained from WT (a) and G24D mutant (b) ClC-2 at indicated pH values. (c,d) Mean ClC-2$_{WT}$ (c) and ClC-2$_{24Asp}$ (d) currents measured after 2 s as function of voltage and pH. n=3-6 ooyctes, error bars, SEM. (e) Currents at -80 mV (~ resting voltage of glomerulosa cells) from ClC-2$_{WT}$ (filled circles) and ClC-2$_{24Asp}$ (open circles) normalized to respective currents at -120 mV at pH 7.4. Note the large pH-dependence of WT currents, which is strongly reduced, but not abolished, by the Gly24Asp mutation.

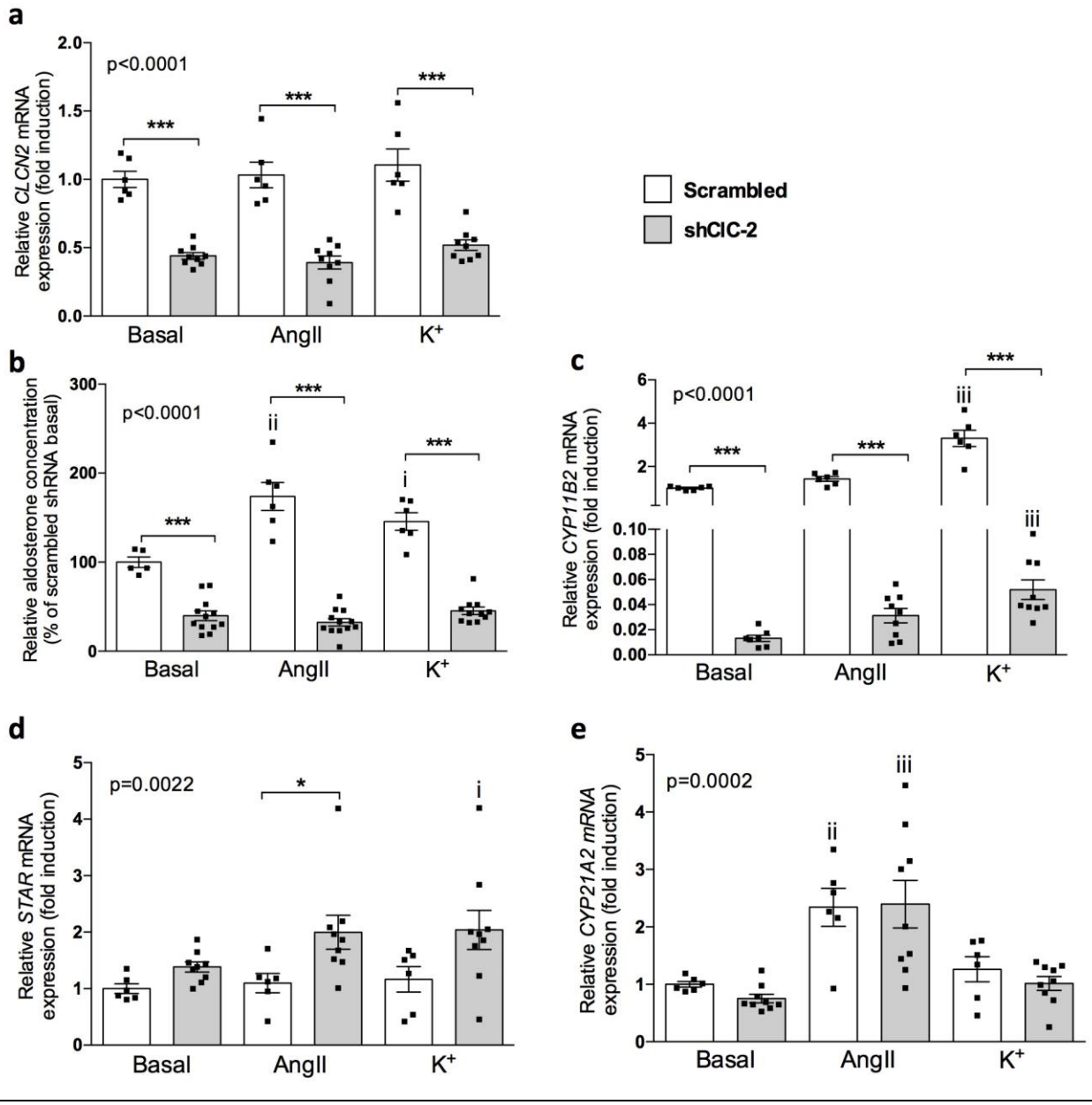

Supplementary Figure 2

Effect of ClC-2 down-regulation on aldosterone production and expression of genes involved in aldosterone biosynthesis.

(a) Basal and stimulated (AngII or K+) mRNA expression of *CLCN2* in H295R-S2 cells infected with scrambled (open bars) or ClC-2 shRNA (filled bars) (1 way ANOVA, p<0.0001, F=28.11). (b) Basal and stimulated aldosterone production by H295R-S2 cells infected with scrambled or ClC-2 shRNA. (c-e) Basal and stimulated mRNA expression of *CYP11B2* (c) (1 way ANOVA, p<0.0001, F=84) *STAR* (d) (Kruskal-Wallys p=0.0022), and *CYP21A2* (e) (Kruskal-Wallys, p=0.0002) in H295R-S2 cells transfected with scrambled or ClC-2 shRNA. Results of mRNA expression are represented as fold induction of cells infected with scrambled shRNA in basal conditions. Values of all experiments are represented as mean ± SEM of two independent experiments performed in experimental triplicates for each condition, (n=6 for scrambled shRNA, n=12 for ClC-2 shRNA). * p<0.05; *** p<0.001; i) p<0.05 stimulated vs basal condition, ii) p<0.01 stimulated vs basal condition; iii) p<0.001 stimulated vs basal condition.

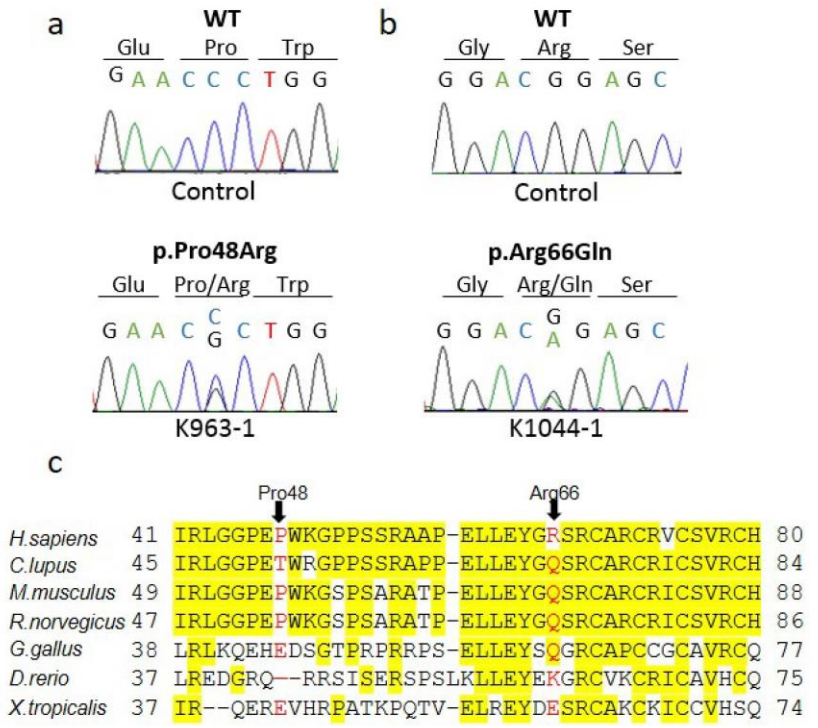

Supplementary Figure 3

***CLCN2* variants identified in subjects with bilateral adrenal hyperplasia.**

(a) Sanger sequencing chromatograms showing the *CLCN2* wild-type sequence and the CLCN2 variant c.143C>G (p.Pro48Arg) identified in the subject K963-1 with bilateral adrenal hyperplasia. (b) Sanger sequencing chromatograms showing the *CLCN2* wild-type sequence and the CLCN2 variant c.197G>A (p.Arg66Gln) identified in the subject K1044-1 with bilateral adrenal hyperplasia. (c) Alignment and conservation of residues encoded by ClC-2 orthologs. Residues that are conserved among more than 3 sequences are highlighted in yellow.

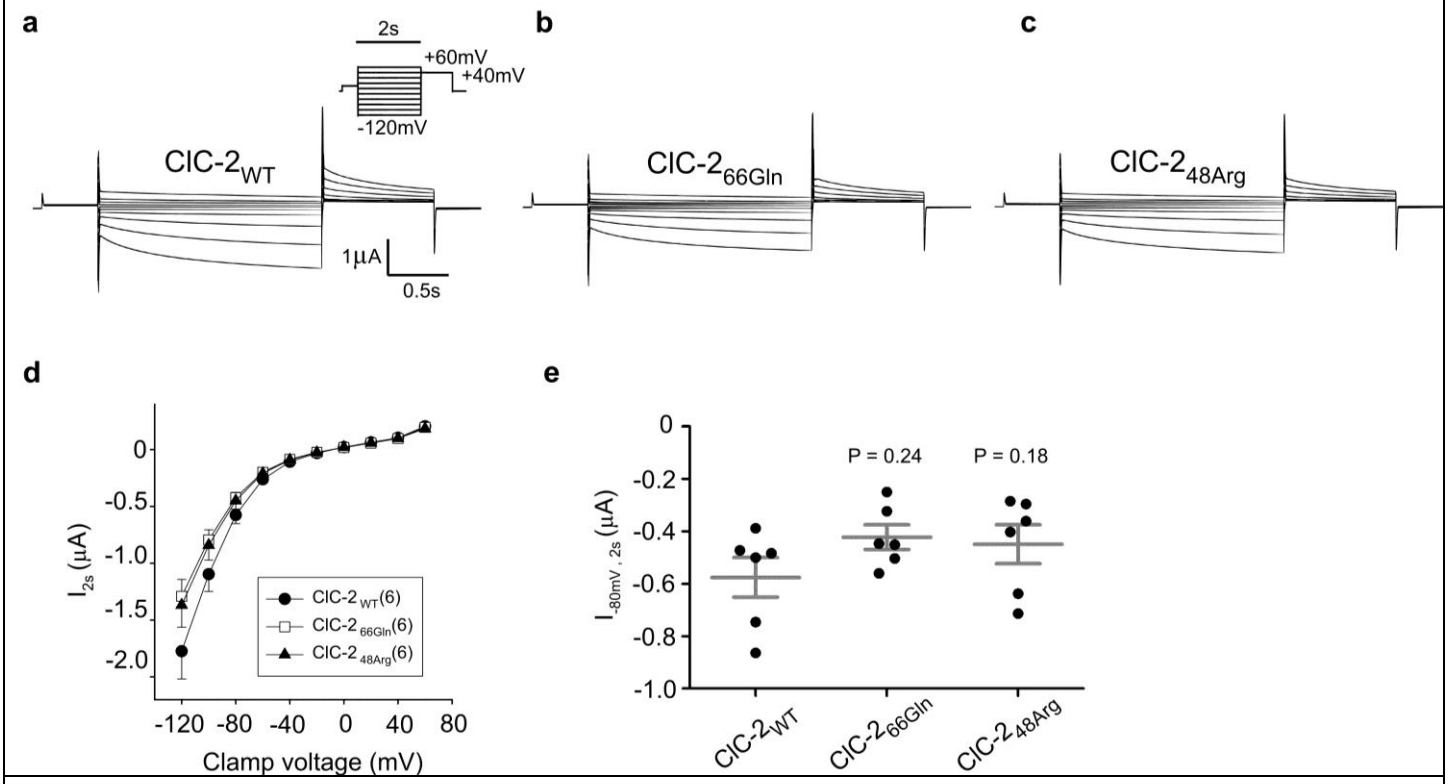

Supplementary Figure 4

Electrophysiological analyses of ClC-2_{66Gln} and ClC-2_{48Arg} channels.

(a-c) Representative chloride current traces measured by two-electrode voltage-clamp from *Xenopus* oocytes injected with 9.2 ng of either human ClC-2_{WT} (a), ClC-2_{66Gln} (b), and ClC-$_{248Arg}$ (c) cRNA. (d) Mean ± SEM currents measured after 2s from experiments in panels (a-c) plotted as a function of clamp voltage. Number of cells, obtained from two different batches of oocytes, indicated in parenthesis. (e) Summary of Cl^- currents at -80mV and after 2s for panels (a-c). Statistical analysis for ClC-2_{66Gln} and ClC-2_{48Arg} were compared with ClC-2_{WT}, Mann-Whitney test.